DOI: 10.4408/IJEGE.2018-01.S-03

VALIDATION OF SWASH MODEL FOR RUN-UP PREDICTION ON A NATURAL EMBAYED BEACH

Leonardo DAMIANI, Alessandra SAPONIERI & Nico VALENTINI

DICATECh - Technical University of Bari – via Orabona, 4 - 70100 Bari, Italy
Corresponding author: leonardo.damiani@poliba.it

EXTENDED ABSTRACT

Attualmente, gli eventi estremi di mareggiata rientrano tra i processi responsabili dell'alterazione dello stato dei litorali e dell'inondazione delle aree costiere, recentemente aggravati dall'innalzamento del livello medio del mare indotto, sia a scala globale che locale, dai cambiamenti climatici in atto. Tali fenomeni inducono effetti potenzialmente dannosi sugli ecosistemi e sulla salute dell'uomo, con ripercussioni sia sul sistema sociale che sulle attività economiche. La valutazione del rischio inondazione rappresenta, quindi, un aspetto cruciale al fine di garantire una efficace gestione integrata del territorio costiero. Si impone, dunque, l'utilizzo di strumenti dedicati per una corretta determinazione del rischio costiero, allo scopo di sviluppare efficienti politiche di mitigazione, protezione e prevenzione, basate su modelli predittivi affidabili, sistemi di allerta rapida e mappe di vulnerabilità, utili al fine di prevenire condizioni spesso irreversibili. In tal senso risulta prioritario definire un programma di monitoraggio ben strutturato e continuo dei litorali, da implementare all'interno di una strategia di gestione costiera nel lungo periodo. In questa prospettiva, i sistemi video rappresentano una soluzione in via di diffusione e di largo utilizzo in tutto il mondo nelle strategie di monitoraggio costiero, poiché permettono un'elevata frequenza di campionamento temporale e spaziale dei processi costieri, con bassi sforzi logistici e costi complessivi di installazione e manutenzione.

Nel presente lavoro viene brevemente descritta l'implementazione e la configurazione di un nuovo sistema di video monitoraggio installato in Puglia, orientato ad alcune caratteristiche fondamentali quali la rapida installazione, robustezza, basso costo, efficienza delle fasi di acquisizione e della catena di elaborazione dei dati, attraverso l'installazione di due stazioni. Il progetto del sistema si pone l'obiettivo principale di ottenere uno strumento in grado di operare in maniera quasi esclusivamente automatica. Il sistema consente l'elaborazione delle immagini acquisite, la geo-rettifica, l'estrazione della linea di riva e l'archiviazione dei risultati in tempo reale su un portale web di dominio pubblico (http://91.121.30.84/). Il sistema è principalmente finalizzato al monitoraggio dei processi di morfodinamica della zona di riva, ma è stato anche ben predisposto per la misura dell'idrodinamica sottocosta. A tal fine, quindi, è stato implementato un tool di gestione composto da una serie di routine supportate da un applicativo web, finalizzate all'elaborazione di immagini (e.g. estrazione linea di riva e geo-rettifica), all'analisi ed alla condivisione dei dati sullo stato attuale della spiaggia e della sua evoluzione, quasi in tempo reale.

Presso la baia di Torre Lapillo (Porto Cesareo, Lecce) il sistema è stato utilizzato per la raccolta di dati di run-up indotto dal moto ondoso sulla spiaggia, utilizzando immagini *time-stack*. I dati raccolti hanno offerto la possibilità di analizzare la sensitività di un modello ad elevata risoluzione per simulare l'interazione di un campo d'onde irregolari con la spiaggia fino alla risalita stessa delle onde, comunemente utilizzato per la risoluzione delle NLSWE. L'approccio numerico si basa sull'accoppiamento del modello spettrale SWAN (Booij *et alii*, 1996) ed il modello non-idrostatico SWASH (Zijlema *et alii*, 2011), utilizzando come forzanti al contorno i risultati in forecasting del modello MeteOcean, sviluppato dal Dipartimento DICCA dell'Università di Genova (Mentaschi *et alii*, 2015), al fine di modellare con elevata precisione le onde a differenti scale spaziali, fino alla dissipazione energetica nella swash zone. Le stime di run-up confrontate con le osservazioni da video-analisi dimostrano di essere in grado di rappresentare fedelmente la zona di swash, avendo ottenuto bias nel calcolo del $R_{2\%}$ pari a circa 5 cm ed un errore quadratico medio di circa 8 cm, entrambi in linea con l'accuratezza complessiva della restituzione topografica in uso. Al fine di risolvere la topo-batimetria del sito, l'area di studio è stata oggetto di diverse campagne di campo. E' stato dimostrato come la particolare conformazione topografica tipica degli ambienti costieri, sia adatta ad essere risolta mediante immagini acquisite da drone (UAV). Utilizzando l'algoritmo *Structure from Motion* (SfM) è stato infatti possibile ricostruire il Modello Digitale di Superficie (DSM), ottenendo una risoluzione a terra pari a 1.5 cm. Viene di seguito descritta brevemente l'elaborazione dei dati e la validazione della metodologia utilizzata, per la quale ci si è avvalsi, inoltre, di dati derivanti da rilievi effettuati mediante metodi tradizionali, quali d-GPS e *Multibeam*. In definitiva, la metodologia proposta può essere utilizzata al fine di creare un tool predittivo per stimare il rischio da inondazione in diverse aree sensibili della costa, come quella pugliese già notoriamente esposta a rischi di erosione avanzata.

ABSTRACT

The work presents the evaluation of performance in wave run-up predicting of the well-known numerical model SWASH (Zijlema *et alii*, 2011), used to reproduce the swash zone hydrodynamics of a natural embayed beach. Field data collected at the bay of Torre Lapillo (Lecce, Italy) by means of video-analysis techniques are used for such purpose. A new automated coastal remote video-monitoring system has been recently installed in collaboration with the Apulian Basin Authority (AdBP), allowing image processing and geo-correction, shoreline extraction and results storage in real time on a public web portal.

The model-numerical chain is based on coupling different models, starting from waves predicted by the MeteoOean model (Mentaschi *et alii*, 2015) up to a one-way nesting of 2D SWAN-SWASH models, in order to obtain an accurate representation of wave processes from deep to shallow waters. The topographic input derives from the combination of different surveys performed by means of Multibeam probe and GPS d-RTK together with a DSM reconstructed from an Unmanned Aerial Vehicle, resulting in a submerged as well as emerged digital model with a high resolution of about 0.015 m. Results show a good agreement between the measured and the simulated values, and confirm the possibility of reconstructing, even on non-instrumented beaches, the hydrodynamics of the nearshore area by numerical means. Simulations are performed with the default empirical coefficients as documented for the model, and a sensitivity analysis is presented on the key wave-breaking parameters (α, β) and the minimum depth threshold (δ), in order to optimize them to most accurately reproduce the observations.

Keywords: *run-up, coastal video monitoring, SWASH model, UAV, MeteOcean wave database*

INTRODUCTION

In 2007 the EU Floods Directive (2007/60/EC) on flood assessment and management entered into force, requiring Member States to identify and map river basins and associated coastal zones where potential flood exists, in order to plan risk management strategies and reduce the probability of flooding and its negative effects on the environment, human health, cultural heritage and economic activities (e.g., Di Risio *et alii*, 2017, Giordano *et alii*, 2017). The Directive also includes coastal floods due to storm surges and tsunamis, recently intensified by climate changes. Sea-level rise has been revealed to be a major effect of climate change (Mimura, 2013), leading to an exacerbation of inundation in addition to exceptional sea levels caused by storm surges, which has become more intense and frequent and, hence, more dangerous for coastal zone, especially for those countries located in low-lying areas.

Such negative effects thus invoke the need for the improvement of new tools concerned with coastal risk management and safety issues, aimed at developing effective mitigation policies, based on reliable predictive models, Early Warning Systems and vulnerability maps, in support of preventing often-irreversible conditions. Moreover, storms induce extensive changes of coastal topography, including shoreline withdraw, destruction of protective dunes and creation of large over-wash deposits. Forecasting such coastal topographic changes relies on determining the nature of storm-induced interactions between topography and hydrodynamic processes.

Run-up estimation from records or forecasted data plays, hence, a relevant role in the identification of flood prone areas. Different tools are available to predict wave induced run-up on beaches as well as structures, in different conditions, based on benchmark data derived from both laboratory and field measurements, including empirical formulations or numerical modelling. Empirical formulations, largely used in engineering practice, allow to assess the run-up elevation, with relative simple procedures, without the need of sophisticated methods. Even though empirical formulas are based on several and different case studies, results are highly dependent from beach foreshore slope and the wave height used as input. In operational forecasting, numerical modelling is typically applied, since it allows to solve non-linearity between variables affecting both hydrodynamics and morphodynamics. Especially in the swash zone, such models, have become robust and efficient tools able to predict beach response to storms and waves transformations, with reasonable computing times. As for empirical formulations, such models like as SBEACH (Larson & Kraus, 1989), XBeach (Roelvink *et alii*, 2009), SWASH (Zijlema *et alii*, 2011), CSHORE (Johnson *et alii*, 2012), although have been largely validated on both prototype and laboratory case studies, need always to be verified when applied to a new area under study. This requires detailed field measurements or aerial and satellite images, which are expensive and weather conditions-dependent.

In recent years, there has been an increasingly widespread use of video systems, enabling a long-term and automated monitoring of coastal areas (e.g. Davidson *et alii*, 2007), with relative low installations and management costs. New video-analysis methodologies, address at structuring an effective tool for coastal area management (Holman & Stanley, 2007; Salmon *et alii*, 2007), have allowed to use data collected from video recordings for calibrating models for wave run-up and rip current occurrence (e.g. Stockdon *et alii*, 2006; Aagard & Holm, 1989). The accuracy of numerical results also depends on topographical input data available, in terms of both submerged and emerged beach profiles, and particularly important in the shallow waters area where the propagation and dissipation phenomena have to be solved accurately, taking also into account other natural factors such as the presence of density stratification (e.g. Fisher *et alii*, 1979), current, vegetation and wave-structure interaction (e.g. Celli *et alii*, 2018).

The present work reports a comparison and sensitivity analysis addressed at assessing performance in run-up prediction of the relative new non-hydrostatic model SWASH. Run-up measurements derive from a video monitoring system recently installed at Porto Cesareo beach (South Italy), where also tide measurement are available are used to validate the model. Moreover, the procedure used to obtain a high-resolution topographic input is briefly described, since different field surveys have been performed and joint in the post-processing.

MATERIAL AND METHODS

Study area

The study area is located in the middle of the embayed bay of Torre Lapillo, a hamlet of Porto Cesareo (Lecce, Italy, Fig. 1). The protected marine area of Porto Cesareo arose from the sub-environment typical of the low coasts, characterized by calcarenitic and sandy rocky beaches. The sandy beaches, varying in width from 10 to 20 m, are characterized by a diameter D_{50} equal to about 0.47 mm and D_{95} to 1.38 mm. Since the early 1960s, both natural processes and anthropic intervention has led to considerable damages on the shore, particularly on the dune system. More recently, a strong erosive trend has been detected, in the period 2009 - 2011, exacerbated by the mean sea level rise, locally up to around 13 cm, also amplified by significant storm events (AdB-Puglia, 2015). Accordingly, a general shoreline withdraw is observed, even equal to about 10 m, especially in the SSE. In terms of the wave climate, using the transposed observations of the nearest buoy (Taranto) recorded in the period 2006-2013, waves come largely from SSE (49.7%) and 34.8% from SO. Summarizing, the wave climate in the area is moderate to low, with an annual height of less than 0.75 m for 44% of observations, while for 12.2% range in the interval $0.75 \le H_s \le 1.75$ m only 0.66% of the records has $H_S \ge 3.0$ m (AdB-Puglia, 2015). The peak period T_p ranges in the interval 3÷5 s for about 32% of observations.

In December 2015, at Torre Lapillo, a video monitoring system has been installed within the Apulian meteo-oceanographic network, managed by the ex. Apulian Basin Authority (AdBP), in order to quantify shoreline erosive trend and beach width reduction (Valentini *et alii*, 2017a). The system consists of two cameras placed on a steel pole, fixed on the roof's parapet of a beach resort (Bacino Grande) at 7.5 m above the mean sea level. The two cameras are oriented in the NO and SE direction, having an angular field of view equal to 51.6° and 56.2°, respectively. Both are Axis, mod. Q1765-LE, equipped with progressive RGB CMOS sensor, which allows 1080p HDTV video recording.

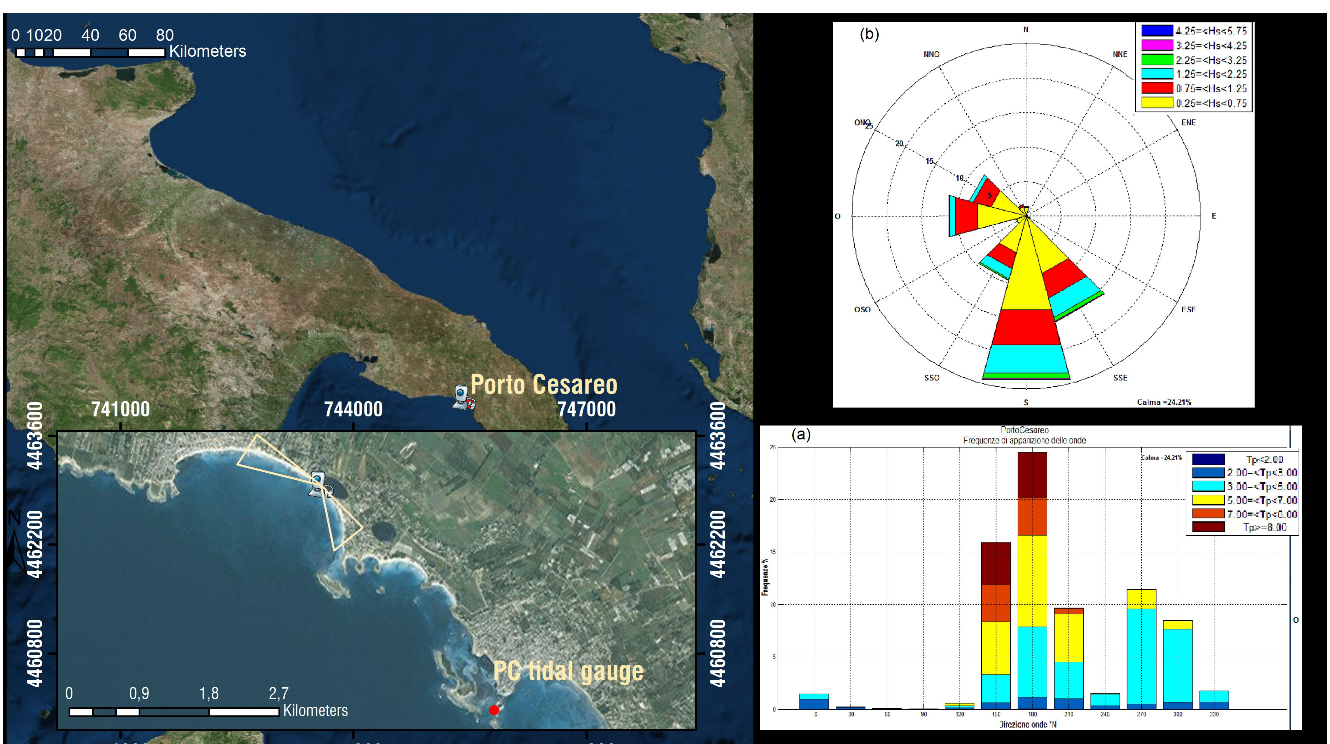

Fig. 1 - Geographical localization of the site study with web-cam location and approximate Field of View (FoV). Nearest tidal buoy (red dots) of Apulia monitoring network. Wave classification according to wave period (a) and to significant wave height (b) from transposed analysis of Taranto wave buoy (ADB-PUGLIA, 2015)

The system includes a local server, HP ProLiant MicroServer Gen 8, and a D-Link Wireless N150 4G LTE router for data transmission. The accuracy of web-cams in the alongshore direction varies from centimeter to about 14 m, at a distance from the web-cam of 700 m, while the footprint area in the cross-shore direction is generally less than 2 m. The accuracy of the system mainly depends on the pixels footprint themselves, but it is also affected by the calibration, rectification procedures and the stability of the cameras position over time. In order to evaluate the overall accuracy of the new system, 6 Ground Control Points were used, located remotely from the web-cams in the range 10÷300 m. The results show a significant difference in positional accuracy between the cross-shore and alongshore directions with a mean square error (RMSE) of 0.43 m and 5.21 m, respectively (Valentini *et alii*, 2017b).

To date, the development of an Apulian coastal video monitoring network has consisted in the installation of two stations in Torre Lapillo (Lecce) and Torre Canne (Brindisi), aimed at ensuring efficient results by acquiring and processing images in a completely automatic way and, at the same time, simplicity in the installation and maintenance by also guaranteeing low installation as well as management costs.

In that context, a new Shoreline Detection Model has been developed for shoreline detection, starting from oblique Timex images, mainly based on the fully automated segmentation of the different coastal areas framed by the cameras and the extraction of the *dry-wet* interface. The model was calibrated and validated with satisfactory results, using databases from a previous video monitoring system installed in Alimini and the two new stations (Valentini *et alii*, 2017b).

The system is mainly composed of three modules and includes the phases of acquisition and processing of images, analysis and publication of results through a Java-based web interface in order to guarantee an easy dissemination of results (http://91.121.30.84/). The acquisition phase, which takes place in local servers guarantees a decentralized framework, being decoupled from archiving and processing of data (Valentini *et alii*, 2017c). The different routines are automated using Python programming, and mainly OpenCV, flamingo-openearth and Gdal/OSR libraries. Figure 2 shows the installation set-up of the cameras and an example of the comparison between the shoreline manually (marker ∇) and automatically (marker o) extracted by means of the SDM model.

Run-up observations

For the purposes of the present study, observed run-up time series are extracted at 16 alongshore locations, by using timestack images. The time on x-axis and the cross-shore distance on the y-axis feature these images for a significant event, dated 11/05/2016. The video used for the generation of the time-stack has a duration of 30 minutes and a frame-rate of 5 Hz. The geo-rectification phase is applied after an appropriate camera distortion correction. The horizontal resolution in the direction across the beach is in the range of 2÷15 cm. Figure 3a shows the FoV of the webcam used for this study and an example of a cross-shore transect with the related time-stack, where the automatically identified extremes are also highlighted.

For timestack images processing, an open source interface was used, developed in MATLAB, "GUI timestack" (https://sourceforge.net/projects/guitimestack/), useful for automatically extracting edge and processing run-up values (Vousdoukas *et alii*, 2012). The obtained pixel values, which represent the cross-

Fig. 2 - Installation set-up of the cameras (a) and example of a comparison between a shoreline manually (V) and automatically (o) extracted by means of the SDM model (b)

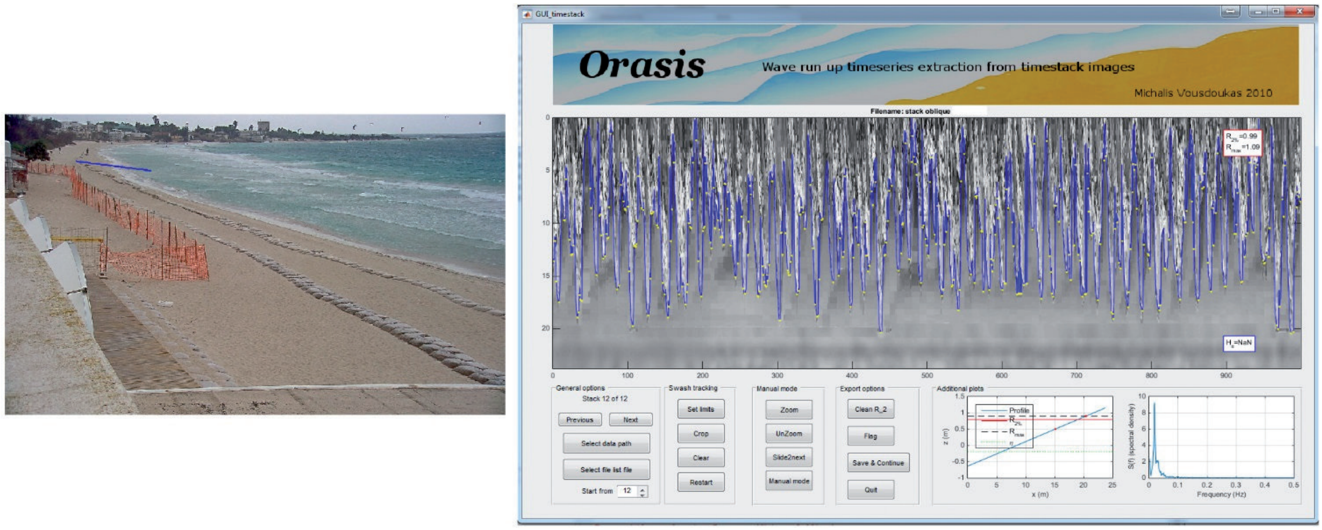

Fig. 3 - Non-distorted oblique FoV of webcam with an example of cross-shore transect (bold line) (a). Processing of timestack trough the GUI (b)

shore coordinates of the swash extremes, are converted into time series of water elevations, using topographic information. The elevations estimated by this method represent the total wave run-up $\eta_{tot}(t)$, which can be described as follows:

$$\eta_{tot}(t) = \eta_{tide} + \eta_{su} + \eta_s + S_{SW}(t) \qquad (1)$$

where η_{tide} and $\eta_{su}(t)$ correspond to the contribution of tide and storm surge, respectively, η_s the maximum set-up, whereas $S_{SW}(t)$ expresses the contribution of swash fluctuations. The run-up elevation R is generally taken as a discrete time series derived from the peaks of the water level fluctuations on beach face, with respect to the mean water level, *peak* $[\eta_s + S_{SW}(t)]$. Given the short distance of the tide gauge from the study area (around 2 km), the excursions η_{tide} and η_{su} have been assumed as known since directly measured. The run-up statistics are then calculated in terms of R_{max} and $R_{2\%}$.

Numerical approach

The numerical approach used in this context is based on the use of the wave prediction database, MeteOcean (Mentaschi *et alii*, 2015), combined with the SWAN model for a detailed simulation of the propagation phenomena and finally, the SWASH non-hydrostatic model to solve the Non-Linear Shallow Water Equations (NLSWE) in the nearshore up to the swash zone.

In the present study, the SWAN model (Booij *et alii*, 1997) is used in a two-dimensional, nonstationary mode, over regular grids, on two domains one-way nested (Fig. 4a). The coarser offshore grid (16.2 km long and 17.4 km wide) starts at a depth of around 90 m, equally discretized in both x-y directions, with a resolution of 150 m. From around 35 m deep water until the shoreline, waves transformations are analysed on a regular finer grid, with a spatial discretization equal to 80. The nearest coastal grid is 4.5 km long and 5.1 km wide.

The boundary conditions are defined in 9 points as spectral parametric inputs (Fig. 4b).

The SWASH model, introduced in Zijlema *et alii* (2011) solves NLSWE, including non-hydrostatic pressure in horizontal momentum equations, with optionally conservative transport of temperature, salinity and suspend sediments. The model uses second order finite difference method, in explicit mode, for staggered grids, whereby mass and momentum are strictly conserved at a discrete level. This simple and efficient scheme is able to track the actual location of incipient wave breaking. The momentum conservation enables the broken waves to propagate with a correct gradual change of a form and to resemble steady bores in a final stage. The Prandtl mixing length hypothesis models the energy dissipation due to the turbulence generated by wave breaking (Guimarães *et alii*, 2015).

In this study, the domain is two-dimensional and one vertical layer is considered for the simulation. The computational grid is curvilinear (205 x 1346) developed in longitudinal direction, having dimensions 203 x 750 m^2, with a finer spatial resolution close to the shoreline, varying in the range 1÷0.13 m.The bottom friction significantly influences wave swash predictions and overtopping for NLSW equation models (Tuan & Oumeraci, 2010), such as SWASH. Therefore, a preliminary sensitivity to bottom friction formulations is investigated, by employing the possible alternative configurations of the model, based on Manning, Chezy, and Colebrook-White values, respectively. The recommended option is based on a constant Manning's roughness coefficient of $n = 0.019$ $(m^{1/2}/s)$. Indeed, we obtain the best performance by using the default option and evaluated an average difference in run-up predictions, by using the other formulations, of 1÷2 cm.

The simulation time was set at 35 min, assuming a spinup time of 5 min, and a temporal discretization of 0.08 s. A simulation of a 35-min length takes approximately 24 hours on a Windows Server, equipped with a 16 cores Intel Xeon E5-2673, up to 2.3 GHz processor, by using mpich2 protocol for parallel MPI implementation. Outputs were requested at the same frequency used for time-stack generation.

In order to faithfully reproduce the topo-bathymetric trend, a high-resolution topographic input has been created from the combination of the Multibeam and d-RTK GPS surveys for the submerged beach and the DSM reconstructed by UAV for the emerged one (res. 0.1 m), both dated 26th May 2016. In this study a multirotor UAV, Aeromax 300 (by Microgeo s.r.l.), supported by a digital camera, Sony α5000, with 20.1 megapixel (Fig. 5a) was used in order to survey a 10,000 m^2 wide area, in the beach portion framed by the SE oriented web-cam.

The images UAV-acquired are at a ground spatial resolution of 0.44 cm. In order to geo-refer the survey, 11 Ground Control Points (GPC) were uniformly distributed on the beach, materialized by A4-size plastic sheets chessboard. In addition, for the quantitative assessment of the UAV survey, 97 Validation Points (VP) were surveyed by using GPS d-RTK (GNSS regional support network), distributed on 16 cross-shore transects, in the same day of the UAV flight. on the beach. The position of the GCPs and the VPs used in this context, together with the DSM generated by the Structure from Motion method (SfM), are shown in Figure 5b, where the dashed boundary line defines the study area. The calculated vertical accuracy, equal to 0.033m, is in good agreement with the absolute precision of the GNSS points (0.013 m) and with previous studies (e.g. Lee *et alii*, 2013, Mancini *et alii*, 2013).

Tracking of simulated run-up

In case of flooding and run-up estimations, SWASH considers a moving shoreline. In the model output options, the horizontal maximum run-up (H_{run}) is defined at the end of the computation as a vector with entries 0 and 1, representing a binary variable for land or water points, respectively. Thus, it is possible to identify the maximum horizontal run-up by $\nabla H_{run} \neq 0$, namely by the grid index corresponding to the last binary values equal to 1. This quantity, combined with the same grid index of the bottom level vector, allows the determination of the vertical maximum run-up. In order to perform a time series analysis, the wet front (wet/dry interface) is tracked by storing the last landward grid index equal to 1 at each time step. The corresponding index of the bottom level is used for defining the time series of run-up vertical excursion. Hence, the value of $R_{2\%}$ is statistically obtained by considering the exceedance curve of the run-up elevations peaks over time. The numerically simulated swash location is then extracted at each cross-shore profile by detecting the shoreward most wet point at a threshold depth δ (here, $\delta = 0.05\ cm$). The sensitivity of swash

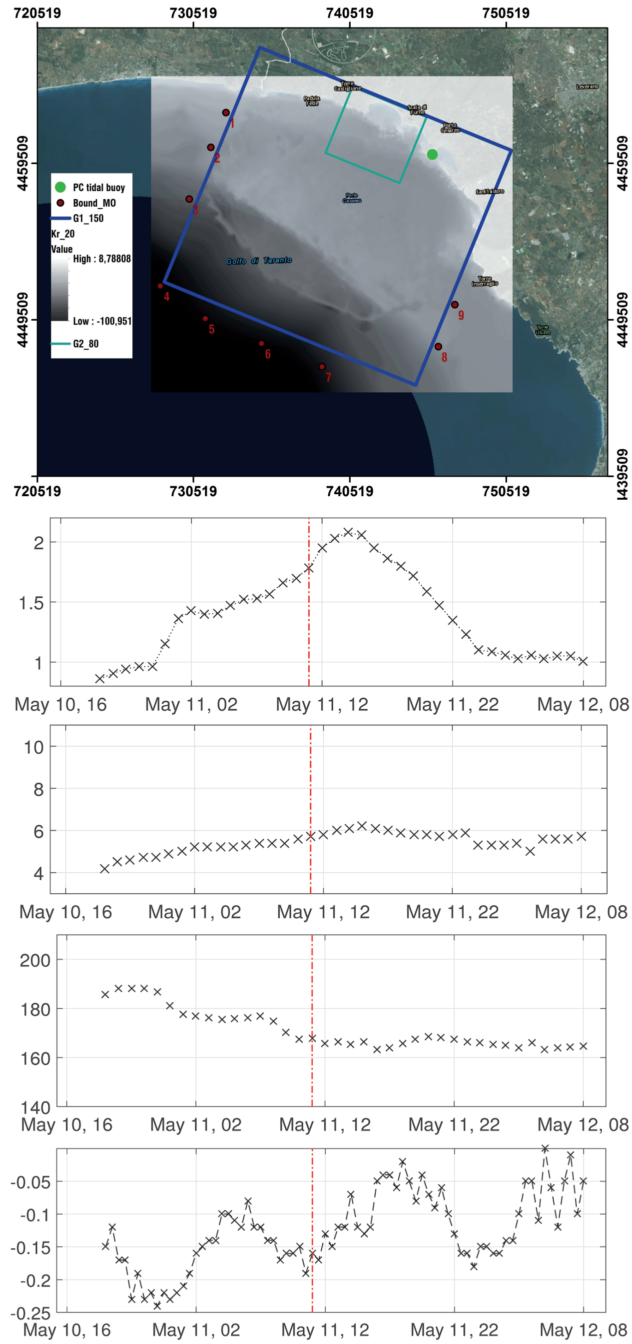

Fig. 4 - (a) Framing of the simulated area: SWAN and SWASH nested grids contours, location of the tidal gauge PC and location of the MeteOcean points used as boundary conditions. (b) Parametric boundary conditions, i.e. at point N. 6 and time series of sea level recorded by tidal gauge PC

measurements to the choice of δ has been described by Holland *et alii*, 1995; Raubenheimer *et alii*, 1995, Stockdon *et alii*, 2014, and herein will be discussed in the following section.

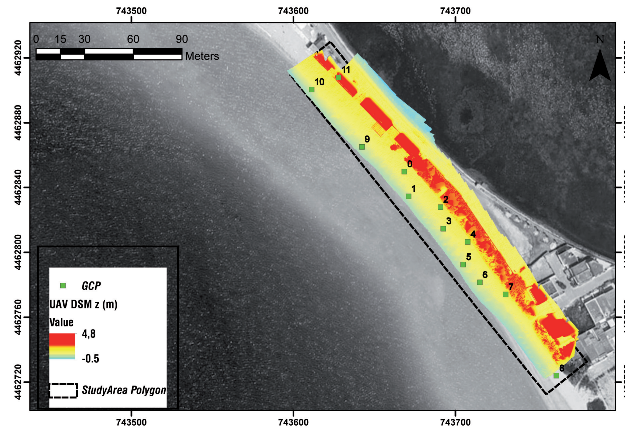

Fig. 5 - UAV Multirotor Aeromax (a). Study area, web-cam position, DSM UAV-derived and location of control and validation points: GCP (squares) and VP (triangles), respectively

RESULTS AND DISCUSSION

Wave swash and run-up

In Figure 6, the comparison between $R_{2\%}$ and R_{max} calculated ($R_{2,sw}$, $R_{max,sw}$) and measured from video-analysis ($R_{2,ts}$, $R_{max,ts}$) is shown in terms of average difference (bias) and of mean square error (RMSE), for the 16 transects investigated, where both estimates are valid.

The maximum difference between the two methods for the two variables considered, $R_{2\%}$ (R_{max}) is 0.182 (0.24) m, the minimum of -0.004 (0.04) m along the selected transects. In general, the $R_{2\%}$ numerical estimates are more in line with the measures than those of R_{max}, the relative RMSE is 0.08 m and excluding transept N.3, the model estimates show a slight tendency to underestimating the measures, as confirmed by the negative value of the bias (-0.06 m). While for $R_{2\%}$ there was no substantial onshore oscillation of the differences, the values of R_{max} in correspondence of the central transects (e.g. 6, 9 and 12) have a more marked underestimation, partly due to the more concentrated presence of geotextiles. In general, the greatest differences were recorded for R_{max}, with the value of RMSE≅0.15 m, on the selected transects.

The general trend is partly motivated by the vertical accuracy of the DSM UAV-derived, for which an almost systematic error of about 0.033 m was evidenced.

Swash parameter sensitivity

The results and analysis presented herein rely on adopting certain assumptions, many of which are derived from the choice of model parameters. Firstly, there is no analytical solution for wave-breaking. Typically, the most used depth-integrated numerical wave models cannot describe overturning of the free surface and thus cannot fully reproduce wave-breaking processes (Cienfuegos *et alii*, 2010; Buckley *et alii*, 2014).

Energy dissipation due to depth-induced wave breaking of the incident band waves in SWASH is modelled by two methods mainly, related to the vertical layer chosen for simulations. The first one is associated to the implementation of a high vertical resolution (layers), where the model can properly determine the dissipation of breaking waves without additional assumptions. Quite similar results have been demonstrated in (Smit *et alii*, 2013) could be obtained with a more computational-feasible low vertical resolution (< 3 layers), by enforcing a hydrostatic pressure distribution at the front of a wave, and locally reducing the non-hydrostatic wave model to simply shallow water equations (hydrostatic).

In this second case, the horizontal region where the so called Hydrostatic Front Approximation (HFA) is activated, varies in time and space mainly affected by two parameters: (i) α, a maximum value of local surface steepness $\partial x\zeta$, in which $\zeta(x,t)$ is the moving free-surface and (ii) β, useful for representing the persistence of wave breaking. Accordingly, the model is set to reduce the criterion based on the value α to β if a neighboring grid point (in both horizontal directions) has been already labelled for hydrostatic computation.

According to Smith *et alii* (2013), the range of α in literature mostly varies from 0.3 (Shaffer *et alii*, 1993) to 0.6 (for multi-layered Bousinnesq model, Lynet *et alii*, 2006). The sensitivity of wave heights to changes in α has been evaluated in Smith *et alii* (2013) and it is demonstrated as under monochromatic wave breaking conditions over sloping beach, the value of 0.6 (used as default in the software), with HFA activated, actually reproduces quite accurately the experiments of Ting & Kirby (1994), for spilling and plunging breakers (less). While, the high-resolution computations applied as well, do not use any information from the experiment. Hence, the default values for both parameters are based on a limited number of tests, primarily laboratory.

In order to evaluate the sensitivity of the model to both the parameters, we first perform runs by changing the β value related to the persistence of breaking in the range 0.3÷0.50, always

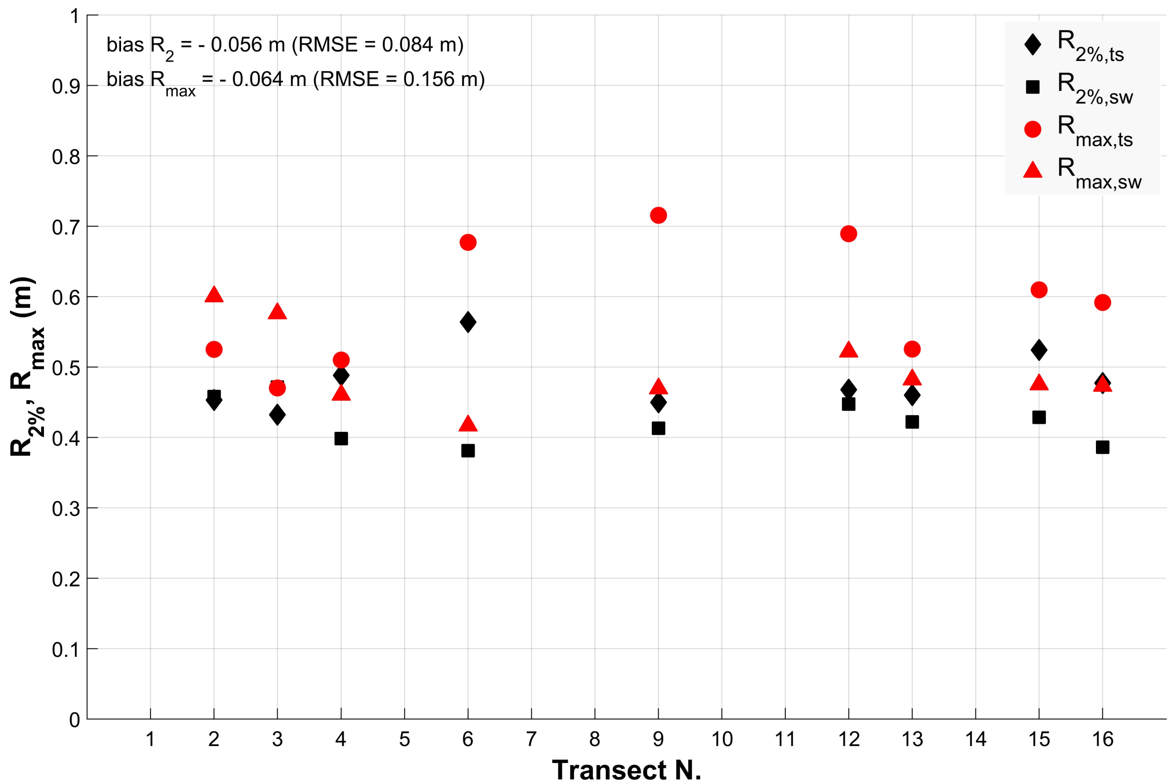

Fig. 6 - Comparison of R%, measured by video monitoring and estimated using SWASH-2D with main statistics correlated (bias and RMSE)

guarantying $\alpha \le \beta$ in the test cases.

In the present, we discuss and present the most representative test cases, in terms of root mean square difference/error (RMSE) and differences [μ (m)].

With respect to both $R_{2\%}$ and R_{max}, the combination of $\alpha=0.6$ and $\beta=0.5$ provided the best fit with the observations, as indicated by lower mean (μ) and RMS differences (Fig. 7a).

In addition to the default value for α, 0.5 and 0.4 were tested.

In these additional sensitivity tests, comparison of 2-d model results to the observed data indicated that lowering this parameter do not offer an improvement over the default breaking value, $\alpha=0.6$.

Run-up sensor depth choice

We investigate moreover the choice of the minimum depth threshold, δ, which is used to extract shoreline water levels (run-up) from the SWASH model, affecting the estimates of swash oscillations. So, the run-up was extracted from all of the simulations by varying the value of δ, analogous to previous tests used for numerical model XBeach (Stockdon *et alii*, 2014). Swash elevations, in term of derived 2% exceedance and maximum run-up, decreased almost logarithmically with increasing δ, as shown in Figure 7b. Moreover, the sensitivity of run-up to δ was found to not substantially differ between the different implementations of SWASH friction formulations.

CONCLUSIONS

In the last decade, the EU Floods Directive (2007/60/EC) on flood assessment and management requests Member States to map areas potentially subject to flood. In coastal areas, risk management invoke the need of prevent and protect areas from negative effects on environment, people and infrastructures derived from storm surges and tsunamis, recently also amplified by climate changes, leading global and local sea level rise and an increasing of storm frequency and intensity. In such a context, the run -up predictions play a relevant role in quantifying the area extension where flood can potentially exist. A new video-monitoring system at Porto Cesareo, installed in the central area of the corresponding embayed beach was used to create time-stack images as run-up observations. In order to solve the complex hydrodynamic interactions, a high-resolution DSM for sub-aerial surface has been implemented. In this sense, the use of non-standard photogrammetric techniques made the input of the UAV images in deriving an accurate and reliable low-cost topographic input, particularly useful for complex sub-environments such as coastal area, where single cross-shore transects do not often guarantee a well representation of the emerged beach. Naturally, some operational constraints are certainly due to the environmental conditions, or to the operational difficulty of GCPs positioning on large and/or irregular surfaces. Run-up

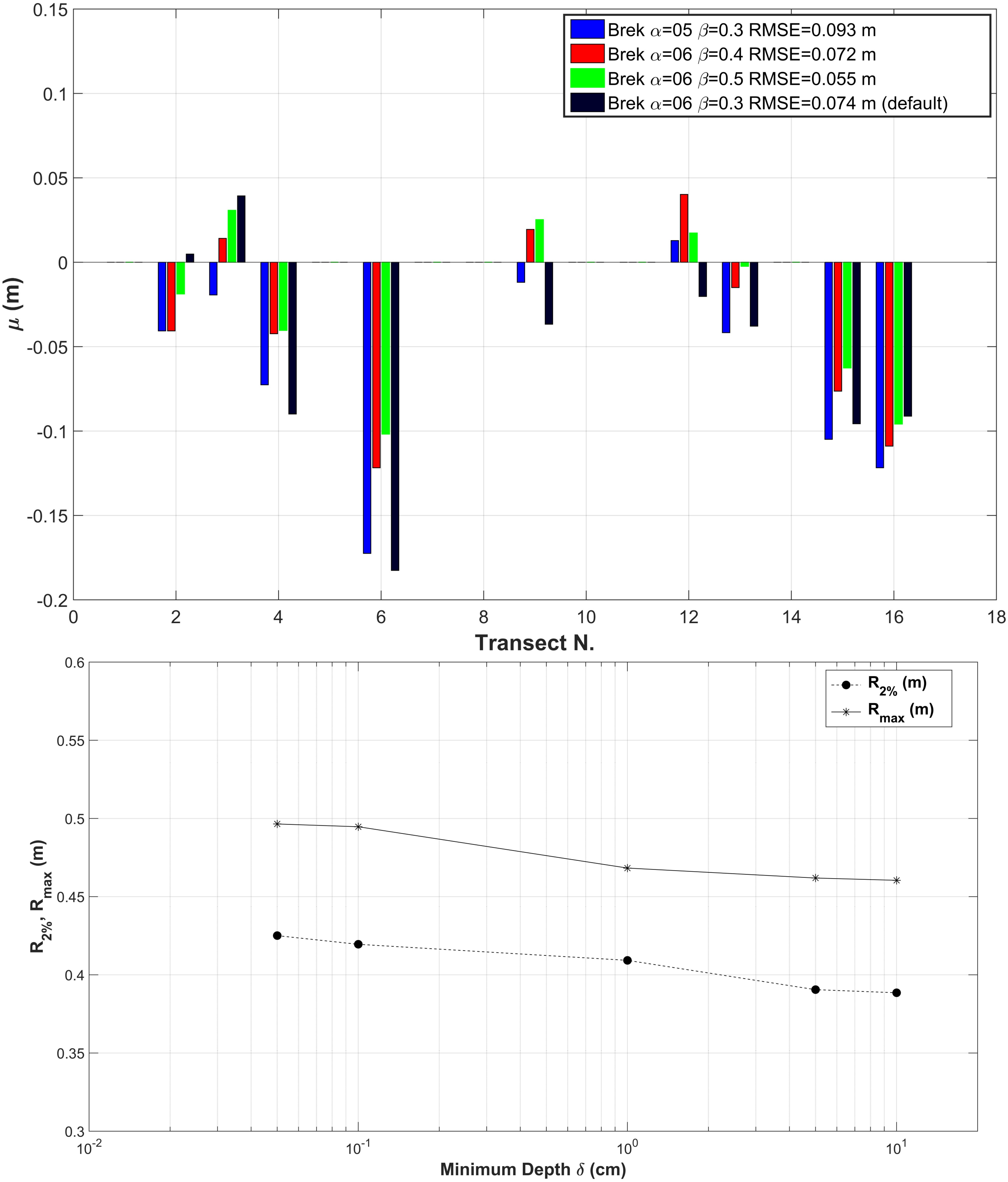

Fig. 7 - Sensitivity of R_2 predictions to variation in the breaking parameter (and) at 16 locations across the surf zone (a). Sensitivity of R_2 (solid lines) and R_{max} (dashed lines) to threshold depth (δ) used to extract runup from 2-d SWASH simulations (b).

numerical estimates compared with video-observations prove they are able to represent faithfully the swash processes. The bias in the calculation of $R_{2\%}$ is equal to -0.056 m and a RMSE of 0.084 m, both almost in line with the overall accuracy of the DSM. Ultimately, this methodology could be used as a predictive tool for the definition of valuable recommendations related to the flood risks on several sensitive areas of the Apulian coast, formerly known to be exposed to leading erosion phenomena. Nevertheless, with tuning of the wave-breaking parameters (α and β) in SWASH, the accuracy of predictions could be further increased substantially (Fig. 7a).

For design purposes, on the other hand, in the definition of maximum run-up elevation, and the consequential potential flooding areas at embayed beach such that, the use of empirical formulations could be often an advantage. However, the drawbacks related to the few number of parameters, which they are based on, and the availability of today high-performance computing processors suggests the need of more advanced and physically-based modelling strategies, such the one presented.

ACKNOWLEDGMENTS

The authors want to thank the Professor G. Frega, who represents a mentor in pursuing our research in Hydraulic and Maritime Engineering. Thanks to Dr. Umiliaco from Microsoft for giving the authors the possibility to use Microsoft Azure for most of the numerical analysis. Intervention co-financed by the Development Fund and Cohesion 2007-2013 - APQ search Apulia Region 'Regional program in support of smart specialization and social and environmental sustainability FutureInResearch'.

REFERENCES

Aagaard T. & Holm J. (1989) - *Digitization of wave run-up using video records.* Journal of Coastal Research, 547-551.

ADB-Puglia (2015) - *Relazione tecnica finale: "Monitoraggio delle dinamiche meteo-marine di controllo dei fenomeni di erosione delle coste".*

Ben Meftah M., Malcangio D. & Mossa M. (2014) - *Vegetation effects on vertical jet structures.* Proceedings of the International Conference on Fluvial Hydraulics, River Flow 20142014, 581-588.

Booij N.R.R.C., Ris R.C. & Holthuijsen L.H. (1999) - *A third-generation wave model for coastal regions: 1. Model description and validation.* Journal of geophysical research: Oceans, **104** (C4), 7649-7666.

Buckley M., Lowe R. & Hansen J. (2014) - *Evaluation of nearshore wave models in steep reef environments.* Ocean Dynamics, **64** (6): 847-862.

Celli, D., Pasquali D., De Girolamo P. & Di Risio M. (2018) - *Effects of submerged berms on the stability of conventional rubble mound breakwaters*. Coastal Engineering, **136**: 16-25.

Cienfuegos R., Barthélemy E. & Bonneton P. (2010) - *Wave-breaking model for Boussinesq-type equations including roller effects in the mass conservation equation.* J Waterw Port Coast Ocean Eng, **136** (1):10-26. Doi:10.1061/(asce)ww.1943-5460.0000022.

Davidson M., Van Koningsveld M., De Kruif A., Rawson J., Holman R., Lamberti A. & Aarninkhof S. (2007) - *The CoastView project: Developing video-derived Coastal State Indicators in support of coastal zone management.* Coastal Engineering, **54** (6): 463-475.

Di Risio M., Bruschi A., Lisi I., Pesarino V., & Pasquali D. (2017) - *Comparative analysis of coastal flooding vulnerability and hazard assessment at national scale.* Journal of Marine Science and Engineering, **5** (4): 51.

Fisher H.B., List E.J., Koh R.C.Y., Imberger J. & Brooks N.H. (1979) - *Mixing in inland and coastal waters.* Academic Press, New York, USA.

Giordano R., Pagano A., Pluchinotta I., Del Amo R.O., Hernandez S.M. & Lafuente E.S. (2017) - *Modelling the complexity of the network of interactions in flood emergency management: The Lorca flash flood case.* Environmental Modelling & Software, **95**: 180-195.

Guimarães P.V., Farina L., Toldo E., Diaz-Hernandez G. & Akhmatskaya E. (2015) - *Numerical simulation of extreme wave runup during storm events in Tramandaí Beach, Rio Grande do Sul, Brazil.* Coastal Engineering, **95**: 171-180.

Holman R.A. & Stanley J. (2007) - *The history and technical capabilities of Argus.* Coastal Engineering, **54** (6): 477-491.

Lynett P.J. (2006) - *Nearshore wave modeling with high-order Boussinesq-type equations.* Journal of Waterway, Port, Coastal, and Ocean Engineering, **1320** (5): 348-357.

Mentaschi L., Besio G., Cassola F. & Mazzino A. (2015) - *Performance evaluation of Wavewatch III in the Mediterranean Sea.* Ocean Modelling, **90**: 82-94.

Lee J.M., Park J.Y. & Choi J.Y. (2013) - *Evaluation of sub-aerial topographic surveying techniques using total station and RTK-GPS for applications in macrotidal sand beach environment.* Journal of Coastal Research, **65** (sp1): 535-540.

Malcangio D. & Mossa M. (2016) - *A laboratory investigation into the influence of a rigid vegetation on the evolution of a round turbulent jet discharged within a cross flow.* Journal of Environmental Management, **173**: 105-120.

Mancini F., Dubbini M., Gattelli M., Stecchi F., Fabbri S. & Gabbianelli G. (2013) - *Using unmanned aerial vehicles (UAV) for high-resolution reconstruction of topography: the structure from motion approach on coastal environments.* Remote Sensing, **5** (12): 6880-6898.

Mimura N. (2013) - *Sea-level rise caused by climate change and its implications for society.* Proceedings of the Japan Academy, Series B, **89** (7): 281-301.

Paprotny D., Andrzejewski P., Terefenko P. & Furmańczyk K. (2014) - *Application of empirical wave run-up formulas to the Polish Baltic Sea Coast.* PloS one, **9** (8): e105437.

Roelvink D., Reniers A., Van Dongeren A. P., De Vries J.V.T., McCall R. & Lescinski J. (2009) - *Modelling storm impacts on beaches, dunes and barrier islands.* Coastal engineering, **56** (11): 1133-1152.

Salmon S.A., Bryan K.R. & Coco G. (2007) - *The use of video systems to measure run-up on beaches*. Journal of Coastal Research, **50**: 211-215.

Schäffer H.A., Madsen P.A. & Deigaard R. (1993) - *A Boussinesq model for waves breakingin shallow water*. Coastal Engineering, **200** (3-4): 185-202.

Smit P., Zijlema M. & Stelling G. (2013) - *Depth-induced wave breaking in a non-hydrostatic, near-shore wave model.* Coast Eng, **76**: 1-16. Doi:10.1016/j.coastaleng.2013.01.008.

Stockdon H.F., Holman R.A., Howd P.A. & Sallenger A.H. (2006) - *Empirical parameterization of setup, swash, and runup*. Coastal Engineering **53** (7): 573-588

Stockdon H.F., Thompson D.M., Plant N.G. & Long J.W. (2014) - *Evaluation of wave runup predictions from numerical and parametric models.* Coastal Engineering, **92**: 1-11.

Ting F.C.K. & Kirby J.T. (1994) - *Observation of undertow and turbulence in a laboratory surf zone*. Coastal Engineering, **240** (1-2): 51-80.

Quang T.T. & Oumeraci H. (2010) - *A numerical model of wave overtopping on seadikes.* Coastal Engineering, **57**: 757-772.

Valentini N., Damiani L., Molfetta M.G., & Saponieri A. (2017a) - *New coastal video-monitoring system achievement and development.* Coastal Engineering Proceedings, 1 (35): 11.

Valentini N., Saponieri A. & Damiani L. (2017b) - *A new video monitoring system in support of Coastal Zone Management at Apulia Region, Italy.* Ocean & Coastal Management, **142**: 122-135.

Valentini N., Saponieri A., Molfetta M.G. & Damiani L. (2017c) - *New algorithms for shoreline monitoring from coastal video systems.* Earth Science Informatics, **10** (4): 495-506.

Vousdoukas M.I., Wziatek D. & Almeida L.P. (2012) - *Coastal vulnerability assessment based on video wave run-up observations at a mesotidal, steep-sloped beach.* Ocean Dynamics, **62** (1): 123-137.

Zijlema M., Stelling G., & Smit P. (2011) - *SWASH: An operational public domain code for simulating wave fields and rapidly varied flows in coastal waters.* Coastal Engineering, **58** (10): 992-1012.

Received April 2017 - Accepted November 2017